Anal. Chem. 1994, *66*, 319–326

Characterization of Human Breast Biopsy Specimens with Near-IR Raman Spectroscopy

Christopher J. Frank,[†] Douglas C. B. Redd,[‡] Ted S. Gansler,[§] and Richard L. McCreery*[,†]

Department of Chemistry, The Ohio State University, 120 West 18th Avenue, Columbus, Ohio 43210, Department of Pathology and Laboratory Medicine, Emory University School of Medicine, 1364 Clifton Road NE, Atlanta, Georgia 30322, and Department of Radiology, Section of Interventional Radiology, Hospital of the University of Pennsylvania, 3400 Spruce Street, Philadelphia, Pennsylvania 19104

Breast biopsy samples were examined with Raman spectroscopy with laser wavelengths ranging from 406 to 830 nm. A combination of a single-stage spectrograph, band reject filter, and CCD detector permitted low laser powers and minimal risk of sample radiation damage. Spectra of formalin-fixed human tissue revealed Raman features for lipids and carotenoids. The best defined lipid features were observed for 782- and 830-nm laser excitation, while carotenoid features were strongest in the 488–515-nm range due to resonance enhancement. Comparison of the spectra with those of fatty acid esters revealed that the major lipid component is a derivative of oleic acid. Lipid and carotenoid Raman bands were superimposed on a luminescent background which was less prominent at longer laser wavelengths. A compact, portable, diode laser spectrometer was tested in a clinical setting with fiber optic sampling. The results indicate that substantial biochemical information is available from near-IR Raman spectroscopy and the technique may have clinical applications.

There are many biological applications of vibrational spectroscopy[1,2] and, more recently, some investigations of diagnostic applications in a clinical setting.[3–5] In principle, the molecular information and specificity of vibrational spectroscopy should be useful for monitoring metabolic status or disease states, in some cases noninvasively. Fourier transform infrared (FT-IR) and nearinfrared (near-IR) absorption spectroscopies have been used for analytical, structural, and dynamic investigations of biomedical materials.[6] FT-IR of various tissue samples has provided useful qualitative chemical information provided interference from water absorption can be managed. While both FT-IR and near-IR spectroscopy have been considered for various biological analyses, there is not yet an example of a routine clinical application for either technique.

Raman spectroscopy has been applied successfully to a variety of biological problems, due in part to the weak scattering of water and to the utility of resonance enhancement. Quite sophisticated techniques have been developed, mostly in the visible and UV wavelength ranges, yielding important information about structure, dynamics, and composition of biological systems. Raman spectroscopy has been considered for characterization of biomedical samples,[7] including breast biopsy samples,[4,10] silicone in lymph nodes,[3] arterial walls,[8] and gynecological tract tissues.[9] While these exploratory reports indicate significant promise for clinical applications of Raman spectroscopy, the complexity of most instruments and frequent interference by fluorescent materials have impeded widespread application or any routine diagnostic procedures.

An example of particular relevance is the Raman spectroscopic investigation of human breast biopsy samples. The high concentration of phospholipids and resonance enhancement of carotene derivatives permit useful Raman spectra to be obtained with visible laser excitation. Redd et al.[4] obtained spectra of lipids, carotenoids, and myoglobin with 407-, 458-, 488-, and 515-nm laser excitation and noted decreased contributions of lipids and carotenoids in carcinoma and fibrosis compared to normal tissue specimens. When the laser wavelength is extended into the red and a CCD detector is employed, the increased sensitivity and reduced fluorescence interference permit collection of enhanced spectral information. With a 782-nm laser, it was possible to observe silicone in lymph node tissue.[3]

† The Ohio State University.
‡ University of Pennsylvania.
§ Emory University.

(1) Moore, C. B., Ed. *Chemical and Biochemical Applications of Laser*; Academic Press: New York, 1974–1979; 4 vol.
(2) Tu, A. T. *Raman Spectroscopy in Biology: Principles and Appliations*; John Wiley & Sons: New York, 1982.
(3) Frank, C. J.; McCreery, R. L.; Redd, D. C. B.; Gansler, T. C. *Appl. Spectrosc.* **1991**, *47*, 387.
(4) Redd, D. C. B.; Feng, Z. C.; Yue, K. J.; Gansler, T. S. *Appl. Spectrosc.* **1993**, *47*, 787.
(5) Redd, D. C. B.; Yue, K. T.; Martin, L. G.; Kaufman, S. L. *J. Vasc. Int. Radiol.* **1991**, *2*, 247.
(6) Putzig, C.; Leugers, A.; McKelvy, M.; Mitchell, G.; Nyquist, R.; Papenfuss, R.; Yurga, L. *Anal. Chem.* **1992**, *64*, 270R.
(7) Ozaki, Y. *Appl. Spectros. Rev.* **1988**, *24*, 259.
(8) Baraga, J. J.; Feld, M. S.; Rava, R. P. *Proc. Natl. Acad. Sci. U.S.A.* **1992**, *89*, 3473.
(9) Liu, C. H.; Das, B. B.; Sha Glassman, W. L.; Tang, G. C.; Yoo, K. M.; Zhu, H. R.; Adkins, D. L.; Lubicz, S. S.; Cleary, J.; Prendente, R.; Celmer, E.; Caron, A.; Alfano, R. R. *J. Photochem. Photobiol. B: Biol.* **1992**, *16*, 187.
(10) Alfano, R. R.; Liu, C. H.; Sha, W. H.; Zhu, H. R.; Akins, D. L.; Cleary, J.; Prudente, R.; Cellmer, E. *Lasers Life Sci.* **1991**, *4*, 1.

0003-2700/94/0366-0319$04.50/0

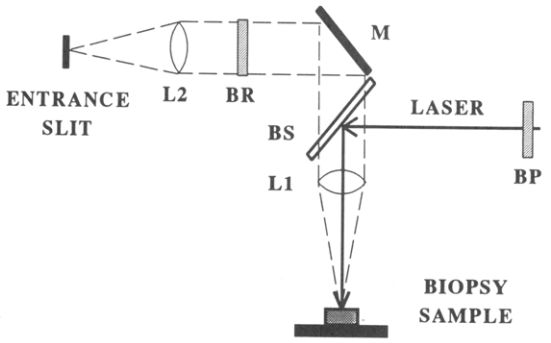

Figure 1. Diagram of system components (side view): L1, 40-mm *f*/3 lens; L2, 30-mm *f*/4 lens; BP bandpass filter; BS 50/50 beam splitter; BR, Rayleigh rejection filter; M, mirror. BP, BS, and BR components are listed in Table 1; the spectrometer and lasers are described in the text.

FT-Raman with a 1064-nm laser has been used to obtain Raman spectra of breast tissue[9,10] and changes in human aorta associated with atherosclerosis.[8]

The objective of the current effort is a detailed characterization of the Raman spectroscopy of normal human breast tissue samples with visible and near-IR excitation. The combination of several recent technological developments resulting in low sample fluorescence from near-IR excitation provides new information about tissue composition. As an initial step toward possible diagnostic applications of Raman spectroscopy, we sought to establish optimal spectroscopic conditions and to identify molecular constituents responsible for major spectral features from normal human breast biopsy samples.

EXPERIMENTAL SECTION

Figure 1 shows the schematic diagram of the apparatus. The spectrograph and CCD were described in detail elsewhere.[3] The Raman spectrometer was based on a single-stage spectrograph (Instruments SA, HR 640) with a 300 l/mm (1.0-μm blaze) grating coupled to a CCD (Photometric CH260 camera head/EEV05-10 CCD with 296 × 1152 pixels, 0.66 cm × 2.59 cm active area). Laser excitation was provided by argon ion, krypton ion, and argon ion pumped Ti:sapphire lasers (Coherent). Table 1 outlines the laser wavelengths used from each laser as well as the optical hardware and conditions used. A bandpass filter (BP), prism with spatial separation, or monochromator was used to remove plasma lines from the gas lasers and nonresonant emissions from the Ti:sapphire laser. An epi-illumination optical configuration providing 180° backscatter collection was used to facilitate rapid changes in the laser excitation wavelength and ease of aligning the samples. The same lens, L1 in Figure 1, was used to focus the excitation laser beam and collect the scattered radiation from the sample. With proper alignment, the laser beam could be made to coincide with the spectrometer slit image at the focal point of the lens. Ideally, the collimated laser beam passed perpendicular to the center of the lens providing overlap of the laser beam and slit image at all distances from the lens. Such a situation allowed signal to be obtained at various distances from the lens with the maximum in signal strength obtained at the focal point of the lens. The operator needed only to adjust the distance of the sample from the lens to bring the sample into optimal focus.

For the experiments reported here, L1 was a 40-mm-diameter achromat (Melles-Griot No. 01 LA O138) with a 120-mm focal length. The excitation laser beam was directed perpendicular to L1 by a 50/50 beam splitter (Melles-Griot). The laser power at the sample varied from 20 to 100 mW (65–320 W/cm^2 with a 200-μm spot size). L1 focused the laser beam onto the sample and collected and collimated the 180° backscattered radiation. The collimated light was then diverted 90° by mirror M and directed through a Rayleigh rejection filter, BR, for the removal of the strong elastic scattering component. The collimated light was focused onto the slit of the spectrograph (*f*/5.6) by L2. L2 was a 30-mm-diameter achromatic lens with a 120 mm focal length (*f*/4) which slightly overfilled the slit and acceptance cone of the spectrograph. L1 and L2 are both 120-mm focal-length lenses providing no magnification of the laser spot image at the slit entrance plane. The Raman shift range was calibrated with known Raman shifts of naphthalene in the 0–1800-cm^{-1} range and with a 50/50 (v/v) acetonitrile/toluene mixture in the 1800–3100-cm^{-1} range. Additionally, all spectra obtained were corrected for the dc offset of the CCD signal and then corrected for the spectrometer response function using a standard white light source correction procedure outlined elsewhere.[12] Briefly, a standard irradiance source (Eppley Labs), calibrated by the manufacturer against NIST standards, was directed through a diffuser into a 200-μm optical fiber cable (C-Technologies). After proper calibration, the fiber optic cable functioned as a specific intensity standard with known intensity as a function of wavelength. For spectrometer response function correction, the fiber was placed at the focal point of the collection lens to mimic the Raman scattering event. Details of the data manipulation are provided later.

Experiments performed with fiber optic sampling were performed with a Raman One spectrograph (Chromex) and a diode laser (Liconix Diolite), as described in detail previously.[11] The spectrograph was coupled to a CCD (Photometrics CH260 camera head, TEK512CB/AR CCD with 512 × 512 pixels, 1.28 cm × 1.28 cm active area). Laser excitation was provided by the 782-nm diode laser operated at 15 °C which provided 7-mW output from the end of the fiber optic probe. The lower power output of the diode laser was compensated by the lower *f*-number and more sensitive spectrometer.[11,12] All components were affixed to a sturdy platform to make the system rugged and portable. Measurements with the portable spectrometer were made at the Emory University Hospital, Department of Anatomic Pathology.

The lipid standards (oleic acid methyl ester, elaidic acid methyl ester, linoleic acid methyl ester, linolenic acid methyl ester) were purchased from Sigma Chemical Co., and naphthalene, acetonitrile, and toluene from Aldrich. Because of their sensitivity to air, the lipid standards were run inside their glass storage ampules.

Normal breast tissue specimens were obtained following surgical excision in patients undergoing reduction mammoplasty, excisional biopsy, or modified radical mastectomy. In

(11) Newmann, C. D.; Bret, G. G.; McCreery, R. L. *Appl. Spectrosc.* **1992**, *46*, 262.
(12) Fryling, M. A.; Frank, C. J.; McCreery, R. L. *Appl. Spectrosc.*, in press.

Table 1. Sources and Optical Components for Raman Spectra Excited with Light of Various Wavelengths

	wavelength, nm						
	406	488	515	647	691	784	830
laser	Kr^+	Ar^+	Ar^+	Kr^+	Ti:sapphire	Ti:sapphire	Ti:sapphire
bandpass filter	Pellin-Broca	Premono-Chromator	Oriel 515 nm	Pellin-Broca	Oriel 691 DF10	Omega 784 nm	Omega 833 DF10
beam splitter	50/50 visible[a]	50/50 visible[a]	50/50 visible[a]	50/50 near-IR[b]	50/50 near-IR	50/50 near-IR	50/50 near-IR
laser rejection filter	Omega 415EFLP	488 Pomfret Research	Kaiser HNF515	Omega 660EFLP	Omega 702REFLP	Kaiser HNF785	830 Pomfret Research
grating order[c]	2	2	2	1	1	1	1
bandpass[d] (cm^{-1})	3.2	2.2	2.0	2.4	2.1	1.7	1.4

[a] Melles Griot (03 BTF 007), optimized for visible range. [b] Melles Griot (03 BTF 015), optimized for near-IR. [c] 300 1/mm grating in ISA 640, blazed at 1000 nm. [d] At 1350 cm^{-1} (25-μm slit).

the two latter groups, tissue provided for spectroscopy was selected from areas near the surgical margins and several centimeters from the tumor prompting the surgical procedures and was documented as normal by a staff pathologist (T.S.G.). All tissue samples were obtained from patients who preoperatively signed an informed consent permitting the investigational use of tissues under guidelines approved by the Human Investigations Committee of Emory University Hospital. To minimize changes in the tissue with time, data presented here were acquired within a 72-h period. Normal breast tissue specimens from 45 patients were examined at 784 nm with 11 of these examined at other wavelengths. All samples were stored in a solution of 10% formalin with 50 mM phosphate buffer (pH 6–7) and run at an ambient temperature of 23 °C.

RESULTS AND DISCUSSION

To demonstrate the changes in the Raman spectra of normal breast tissue with wavelength, spectra were collected at seven excitation wavelengths varying from 406 to 830 nm. For each wavelength different optical components (filters, beam splitter) were employed to acquire Raman spectra, hence, imposing a different spectrometer response function for each wavelength. The spectrometer response function included factors such as lens and filter transmission, spectrograph transmission, and quantum efficiency of the CCD. Correction of the spectrometer response function for each wavelength was necessary in order to obtain an accurate representation of the specimen's Raman spectrum as will be described in Figures 2 and 3. The spectrometer response function was corrected with a procedure employing a calibrated white light source coupled to a fiber optic cable. The procedure involved the acquisition of the sample's Raman spectrum at a given laser wavelength, replacement of the sample by the fiber optic cable, and acquisition of the fiber output spectrum. The corrected spectrum (S_{corr}) is determined from the calibrated white light output via eq 1, as described previously,[12] where S_{obs} and S_f

$$S_{corr} = \frac{S_{obs}}{S_f} L_f \qquad (1)$$

are the observed sample and fiber spectra, respectively, and L_f is the calibrated specific intensity of the fiber.[12] This spectral correction procedure was automated through the use of an integrated PC program which also calibrated the Raman shift axis, thus performing complete spectral calibration in a single multistep operation.

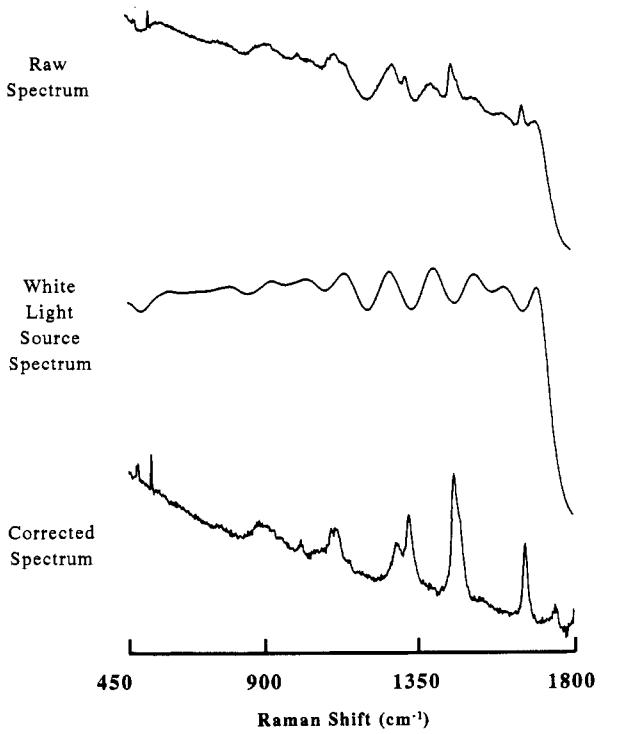

Figure 2. Spectra illustrating the correction of Raman spectra for the spectrometer response function, in particular the filter transmission function. The raw spectrum is the 691-nm Raman spectrum of normal breast tissue obtained using an Omega 702REFLP filter, 40-mW laser power, and 60-s integration time. The white light source spectrum was obtained from the calibrated fiber source, 45-s integration. The corrected spectrum was calculated as described in the text.

Figure 2 demonstrates the correction of the modulation introduced in the 691-nm Raman spectrum of normal breast tissue by the dielectric Rayleigh rejection filter (Omega 702REFLP). In the uncorrected Raman spectrum, features are superimposed on top of a large background due mainly to sample fluorescence. This signal was modulated by the filter transmission, which obscured observation of several bands in the raw spectrum in Figure 2. The fiber optic cable spectrum (White Light Source Spectrum) was acquired, and the raw spectrum was corrected as described above to yield the corrected spectrum in Figure 2. The corrected spectrum illustrates the effective removal of the filter-induced modulation permitting the observation of several Raman bands not otherwise apparent in the raw spectrum.

Experiments performed with near-IR excitation cover a larger wavelength range compared to visible excitation. Hence, near-IR Raman spectra are more affected by changes

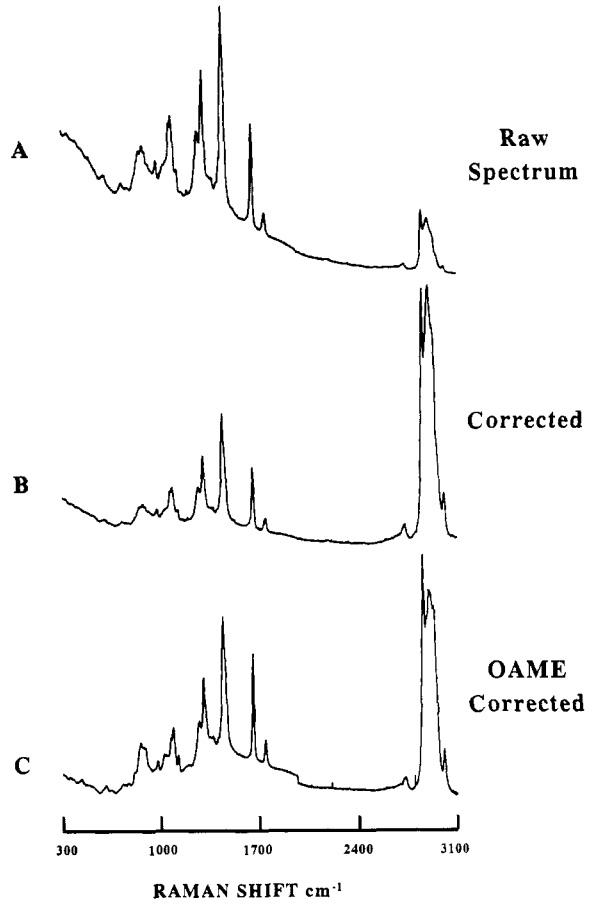

Figure 3. Spectra illustrating the correction of Raman spectra for the spectrometer response function, in particular the changes in detector quantum efficiency with wavelength. Spectra A and B are uncorrected and corrected Raman spectra, respectively, of normal breast tissue obtained with 784-nm excitation (40 mW) and 300-s integration time. Spectrum C is a corrected Raman spectrum of oleic acid methyl ester, obtained in 60 s, with other conditions same as with (A).

in quantum efficiency of silicon-based CCDs, which have a decreasing response in the near-IR region. Figure 3 illustrates the effect of decreasing quantum efficiency on Raman spectra and its correction by the white light standard. Spectra A and B in Figure 3 are the uncorrected and corrected Raman spectra of normal breast tissue obtained with 784-nm excitation. Most striking is the correction of the Raman band intensities in the C–H region, which had been significantly attenuated by the decreasing detector sensitivity. This procedure was very valuable for obtaining accurate relative peak intensities, thus allowing spectral comparisons as the excitation wavelength was varied. The observed Raman shifts from the 784-nm Raman spectrum of normal breast tissue are shown in Figure 4 with the vibrational assignments for each band reported in Table 2.

The use of red and near-IR excitation provided a Raman spectrum of normal breast tissue that was different from that obtained with visible excitation. To characterize the differences, Raman spectra were acquired from the same tissue specimens as the excitation wavelength was varied from 406 to 830 nm. Figure 5 illustrates these changes using excitation wavelengths of 406, 488, 515, 647, 691, 784, and 830 nm. An obvious difference in these spectra is the change in the magnitude of the background luminescence with spectra acquired with 406-, 488-, and 515-nm excitation on the increasing side of the fluorescence background. Raman spectra acquired with 647- and 691-nm excitation are on the decreasing side, and at 784 and 830 nm, spectra were either off the fluorescence envelope or on its weak wings. Others have noted a maximum in the fluorescence envelope at ca. 530 nm with both fluorescence and Raman spectroscopy.[4,13,14] For normal breast tissue and oleic acid methyl ester, Figure 6 illustrates the change in the Raman intensity, R, of the 1439-cm^{-1} band measured above background compared to the background intensity, F, as measured at 1200 cm^{-1} relative to the excitation wavelength. Tahara and Hamaguchi[15] have used the ratio R/F to evaluate the effective fluorescence interference suppression. The data for Figure 6 show that varying the excitation wavelength from 406 to 830 nm increases the R/F ratio over 2 orders of magnitude, with the near-IR wavelengths (784 and 830 nm) providing the maximum fluorescence interference suppression. The background in normal breast tissue specimens was comprised mostly of fluorescence from tissue components but may have contained other sources such as stray light and nonsample fluorescence. The background intensity was observed to fluctuate from specimen to specimen, and as Alfano has discussed, its nature may reflect a variety of sample differences, including patient age. Alfano, using fluorescence spectroscopy, reported observing a 5-fold increase in the fluorescence intensity for an 80-year-old patient compared to one who was 64.[13] Experimentally, the background fluorescence intensity was observed to decrease slightly within the first few minutes of laser exposure, probably due to photodegradation of photosensitive fluorophores, but with extended laser exposures (>5 min) no additional change in the R/F ratio was observed. Since longer laser exposures (>30 min) led to sample desiccation, long exposures were avoided in the experiments reported here.

A second notable difference in the Raman spectra of Figure 5 is the Raman bands observed with visible or red/near-IR excitation. Table 3 lists the major Raman bands observed at each excitation wavelength and the tissue component attributable to that band. The use of near-IR excitation (784 and 830 nm) clearly permitted the observation of a maximum number of Raman bands. For samples with a large fluorescence background, fewer Raman bands were observed when visible excitation was used than were seen in a sample with a lower fluorescence background. For Raman spectra acquired with near-IR excitation (784 and 830 nm), all major Raman bands were observed regardless of the level of fluorescence background.

Redd et al.[4] have attributed the bands observed in the visible spectra (406–515 nm) of normal breast tissues to vibrations within both lipid and carotenoid tissue components. They identified the three prominent bands in the visible spectra, 1105, 1156, and 1517 cm^{-1}, as characteristic resonance-enhanced Raman peaks of carotenoids. Additionally, these three prominent bands were observed and identified in the 515-nm Raman spectra of noncalcified atherosclerotic lesions, also referred to as fatty plaque, from human coronary

(13) Alfano, R. R.; Tang, G. C.; Pradhan, A.; Lam, W.; Choy, D. S. J.; Opher, E. *IEEE J. Quant. Electron.* **1987**, *QE-23*, 1806.
(14) Alfano, R. R.; Pradhan, A.; Tang, G. C.; Wahl, S. J. *J. Opt. Soc. Am. B* **1989**, *6*, 1015.
(15) Tahara, T.; Hamaguchi, H. *Appl. Spectrosc.* **1993**, *6*, 391.

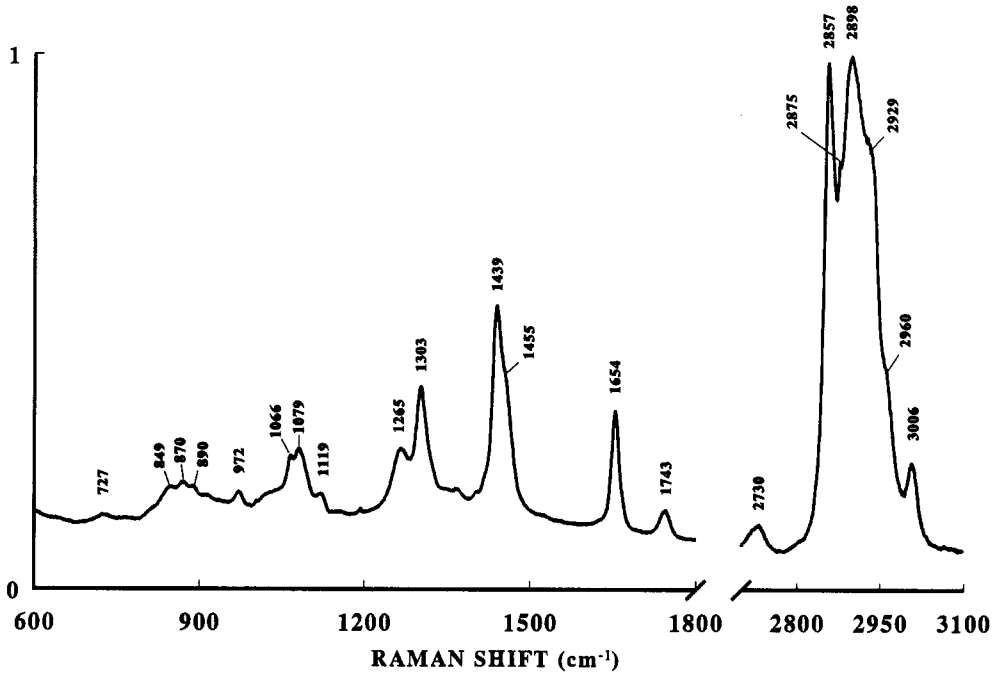

Figure 4. Raman spectrum (784-nm) of normal breast tissue. Laser power was 40 mW at the sample and integration time was 300 s.

Table 2. Major Raman Band Frequencies (cm^{-1}) of Tissue and Lipid Standards (784-nm Excitation)

breast tissue	OAME[a]	LAME[a]	LLAM[a]	EAME[a]	assignment
3006	3003	3012	3015	2996	=C—H stretch[24,26] [b]
2960	2960	2951	2951	2952	C—H stretch (—CH_3 asym)[25,27]
2929	2929	2924	2935	2928	C—H stretch (—CH_3 sym)[25,27]
2898	2897	2903	2911	2899	C—H stretch (—CH_3 sym)[25]
2875	2876	2877	2880	2879	C—H stretch (—CH_2 asym)[27]
2857	2856	2855	2855	2853	C—H stretch (—CH_2— sym)[25]
2730	2734	2732	2729	2729	
1743	1743	1743	1741	1744	C=O stretch[24,26]
1654	1655	1658	1658	1669	C=C stretch[24,26]
1455	1456	1449	1451	1461	CH_2 deformation[c] [25,27]
1439	1442	1442	1442	1439	CH_2 scissoring deformation[24,27]
1303	1304	1304	1304	1304	CH_2 twisting[24,25]
1265	1268	1266	1267		=C—H in plane deformation[24,26]
		1187	1168		
1119	1118	1111		1120	C—C stretch[25,27]
1079	1082	1076	1085	1085	C—C stretch[25,27]
1066	1067	1066	1070	1067	C—C stretch[25,27]
	1019	1019	1022	1021	C—C stretch[25]
972	973	973	973	968 (vw)	=C—H out of plane deformation[25,26]
890	887	911	940	890	
870	868	882	867	870	
849	856	842		841	
727	728	724	719		=C—H in plane bend[24]
	610	610	608	611	

[a] OAME, oleic acid methyl ester; LAME, linoleic acid methyl ester; LLAM, linoleic acid methyl ester; EAME, elaidic acid methyl ester. [b] References indicate assignments from the literature. [c] Shoulder.

arteries[5,16] and in the 488-nm Raman spectra of carotenoid components contained in low-density lipoproteins isolated from human plasma.[17] The carotenoid bands are not observed in the red to near-IR spectra, implying that the carotenoid components are at too low a concentration to be observed without resonance enhancement. Several other weaker bands due to lipid component vibrations are apparent in the visible Raman spectra. As will be shown later, the red/near-IR spectra (647–830 nm) are comprised of only lipid component bands.

The peak areas of the 1654-cm^{-1} lipid and the 1525-cm^{-1} carotenoid band relative to the 1439-cm^{-1} lipid band are shown in Figure 7 as a function of wavelength. The 1439-, 1525-, and 1654-cm^{-1} band areas were measured above a baseline between 1410 and 1490, 1485 and 1547, and 1635 and 1671 cm^{-1}, respectively. The 1525-/1439-cm^{-1} area ratio shows a maximum with 488-nm excitation and falls off to zero at red and near-IR excitation. This increase in the 1525-/1439-cm^{-1} ratio is due the resonance enhancements of the polyene chain of carotenoids in the breast tissue. This resonance enhancement maximum is consistent with profiles seen for *all-trans* β-carotene in *n*-hexane[18] and in cyclohexane[19]

(16) Clarke, R. H.; Wang, Q.; Isner, J. M. *Appl. Opt.* **1988**, *27*, 4799.
(17) Verma, S. P.; Philippot, J. R.; Bonnet, B.; Sainte-Marie, J.; Moschetto, Y.; Wallach, D. F. H. *Biomed. Biophys. Res. Commun.* **1984**, *122*, 867.

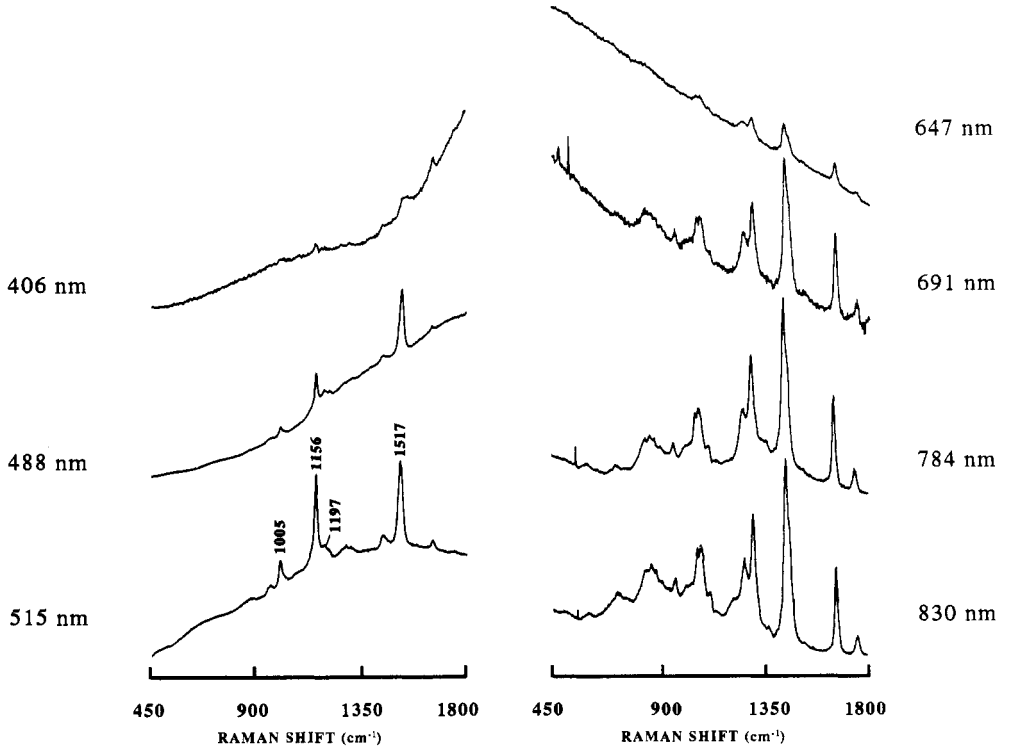

Figure 5. Raman spectra of a normal breast tissue specimen versus wavelength. Spectral conditions are as follows: excitation wavelength, nm (laser power at sample, milliwatts/integration time, seconds) 406 (20/60); 488 (20/30); 515 (50/15); 647 (40/60); 691 (40/60); 784 (40/300); 830 (80/300). Integration times were adjusted to provide maximum signal before CCD saturation. Because of the inefficiency using the grating in second order, visible excitation integration times were longer than for a spectrometer optimized in this region.

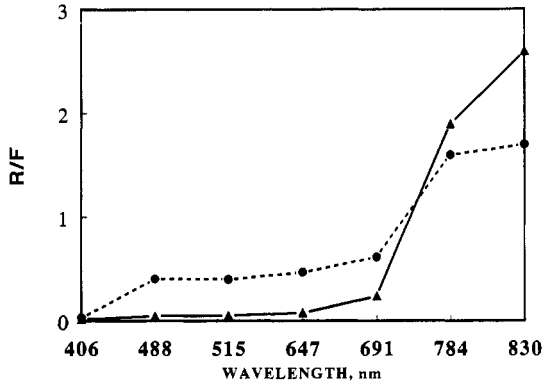

Figure 6. Ratio of Raman intensity to luminescence background (R/F) versus wavelength for normal breast tissue (triangles) and oleic acid methyl ester (circles). R is the 1439-cm^{-1} Raman mode intensity above background; F is the fluorescence background intensity at 1200 cm^{-1}.

Table 3. Major Raman Bands of Biopsy Samples for Various Laser Wavelengths[a]

wavelength, nm							
406	488	515	647	691	784	830	component
					727	727	lipid
	872				870	868	lipid
				972	972	972	lipid
1005[b]	1006	1005					carotenoid
				1065	1066	1065	lipid
			1081	1077	1079	1079	lipid
					1119	1119	lipid
1155	1157	1156					carotenoid
	1190	1197					carotenoid
1263			1269	1265	1265	1265	lipid
1300		1305	1301	1303	1303	1303	lipid
1442	1443	1438	1439	1440	1439	1439	lipid
1526	1525	1517					carotenoid
1654	1653	1654	1654	1655	1654	1654	lipid
				1745	1743	1745	lipid

[a] Missing value indicates that band was not observed. [b] Values reported as Raman shift (cm^{-1}) from laser excitation wavelength.

solutions. The 1654-/1439-cm^{-1} area ratios for both the normal breast tissue and the lipid standard (OAME) are similar and follow the same trend, being fairly constant from 830 nm to 488 nm, followed by a sharp increase with 406-nm excitation. This sharp increase may be due to resonance enhancement of the unsaturation bond in the lipids. Raman spectra reported by Redd et al.[4] showed a similar increase of the 1654-/1439-cm^{-1} intensity ratio when going from 514.5- to 457.9- to 406.7-nm excitation. These data indicate that bands due to lipids are not greatly affected by changes in laser excitation between 488 and 830 nm while those of carotenoids are.

The red and near-IR Raman bands are due to vibrations of lipid components within the tissue specimens. The lipid component giving rise to these bands was determined by comparing the Raman spectra of several C_{18} lipid standards. C_{18} lipid components are known to comprise ~60% of the fatty acids from normal human breast tissue.[21-23] Additionally, the Raman spectra of normal breast tissue show an unsaturation band at 1654 cm^{-1} and a carbonyl stretch at 1743 cm^{-1}. Therefore, methyl ester lipid standards which contained various amounts of unsaturation and contained cis

(18) Rimai, L.; Kilponen, R. G.; Gill, D. *J. Am. Chem. Soc.* **1970**, *92*, 3824.
(19) Saito, S.; Tasumi, M.; Eugster, C. H. *J. Raman Spectrosc.* **1983**, *14*, 299.
(20) Carrabba, M. M.; Rauh, R. D. U.S. Patent No. 5,11,127, 1992.
(21) Hietanen, E.; Punnonen, K.; Auvinen, O. *Carcinogenesis* **1986**, *7*, 1965.
(22) Sakai, K.; Okuyama, H.; Yura, J.; Takeyama, H.; Shinagawa, N.; Tsuruga, N.; Kato, K.; Miura, K.; Kawase, K.; Tsujimura, T.; Naruse, T.; Koike, A. *Carcinogenesis* **1992**, *13*, 579.
(23) Punnonen, K.; Hietanen, O.; Auvinen, O.; Punnonen, R. *J. Cancer Res. Clin. Oncol.* **1989**, *115*, 575.

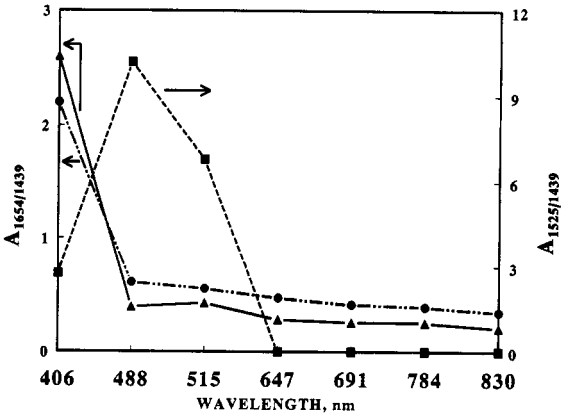

Figure 7. Area ratios of the 1654-cm^{-1} band for normal breast tissue (triangles) and oleic acid methyl ester (circles), and the 1525-cm^{-1} band of normal breast tissue (squares) relative to 1439-cm^{-1} band intensity, all as a function of laser wavelength.

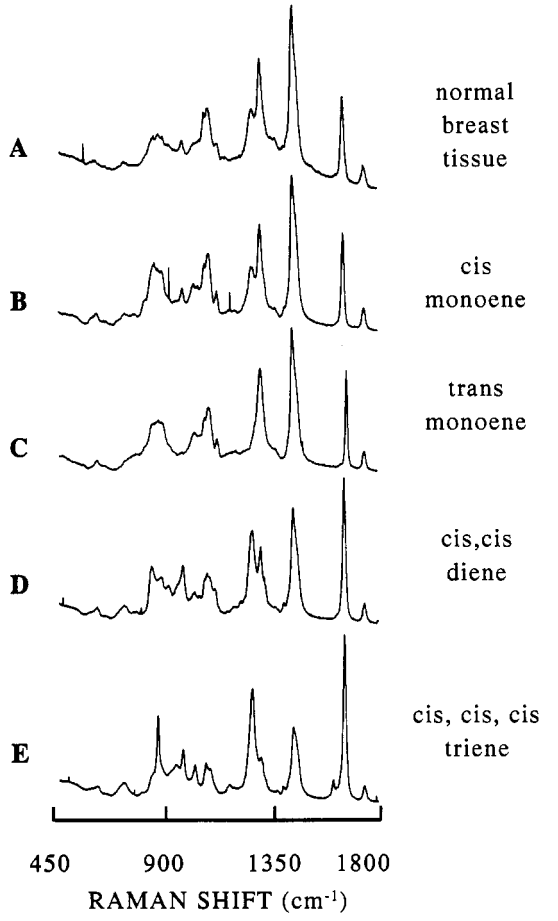

Figure 8. Raman spectra (784 nm) comparing normal breast tissue to the methyl esters of lipid standards: oleic acid (cis monoene); elaidic acid (trans monoene); linoleic acid (cis, cis diene); linolenic acid (cis, cis, cis triene). Spectral conditions were 25-μm slit (1.7-cm^{-1} bandpass) for all spectra. Tissue: 40 mW, 300-s integration. Lipid standards: 100 mW, 180-s integration. Sharp spikes are random hard radiation events, which are seen more frequently in long integrations.

and trans configurations around the C=C bond were examined and compared to spectra of normal breast tissue. Figure 8 shows the Raman spectra of normal breast tissue compared to the methyl esters of the following: oleic acid (cis monoene); elaidic acid (trans monoene); linoleic acid (cis, cis diene); and linolenic acid (cis, cis, cis triene). The observed band positions and their assignments for the spectra shown in Figure 8 are listed in Table 2. The assignments listed are based on a compilation by Tu[25] plus Sahdeghi-Jorabchi et al.,[24] Davies et al.,[26] and Yellin and Levin.[27]

Several observations lead to the determination of the lipid component giving rising to the major Raman features in normal breast tissue. First, the C=C band in the lipid standards was located at ~1654 cm^{-1} for the cis configuration but moves to a higher Raman shift, 1669 cm^{-1}, for the trans configuration. Normal breast tissue shows a C=C bond at 1654 cm^{-1}, suggesting a cis configuration around the double bond. Second, the degree of unsaturation was estimated by comparing the relative intensity of the 1654-cm^{-1} band between lipid standards by using the 1743-cm^{-1} band (C=O stretch) as an internal intensity standard. The 1654-/1743-cm^{-1} intensity ratio increased with the degree of unsaturation. Also, the 1265- and 727-cm^{-1} bands, which are due to =C—H in-plane deformation in unconjugated cis double bonds, increased in intensity with increasing degree of cis unsaturation. Note that the trans lipid standard does not show these bands. The relative intensities of the 1654-, 1265-, and 727-cm^{-1} bands of normal breast tissue relative to the same bands in the lipid standard suggest the lipid component is monounsaturated. Additional evidence supporting the identification of this lipid as the cis monoene form was obtained from the C—H stretch region of oleic acid methyl ester as seen in spectrum C of Figure 3 and the other lipid standards, most notably the C—H stretch band positions and the relative intensity of the 3006-cm^{-1} band (=C—H stretch). Upon further comparison of all the band positions of normal breast tissue and oleic acid methyl ester (OAME) in Table 2, the major lipid component was determined to be an ester of oleic acid. Baraga et al.[8] have attributed the spectral features of adipose tissue surrounding aortic artery samples to the triglyceride triolein, which contains three oleic acid chains.

To evaluate the use of near-IR Raman spectroscopy in a more clinically relevant situation, a portable Raman spectrometer coupled to a fiber optic probe was assembled and transported to Emory University Hospital, Department of Anatomic Pathology. A schematic of the portable spectrometer is shown in the inset of Figure 9. By use of a fiber optic probe, Raman spectra were acquired under the supervision of a staff pathologist (T.S.G.), from normal margins in surgical mastectomy specimens. Figure 9 shows a representative Raman spectrum of normal breast tissue obtained with 782-nm diode laser excitation. The Raman bands seen in this spectrum are the same as those seen in the 784-nm Raman spectrum in Figure 4, except that the two bands labeled SR below 700 cm^{-1} are silica Raman bands generated in the fiber optic probe. Such interference can be significantly reduced or eliminated by appropriate fiber optic probe designs employing Rayleigh rejection filters within the probe tip.[20] Additionally, signal-to-noise ratio can be increased and integration times reduced by employing commercially available higher output (~100 mW) diode lasers.

(24) Sahdeghi-Jorabchi, H.; Wilson, R. H.; Belton, P. S.; Edwards, J. D.; Coxon, D. T. *Spectrochim. Acta* **1991**, *47A*, 1449.
(25) Tu, A. T. *Raman Spectroscopy in Biology: Principles and Appliations*; John Wiley & Sons: New York, 1982; pp 204–5, and references therein.
(26) Davies, J. E. D.; Hodge, P.; Barve, J. A.; Gunstone, F. D.; Ismail, I. A. *J. Chem. Soc., Perkin Trans. 2* **1972**, *2*, 1557.
(27) Yellin, N.; Levin, I. W. *Biochim. Biophys. Acta* **1977**, *489*, 177.

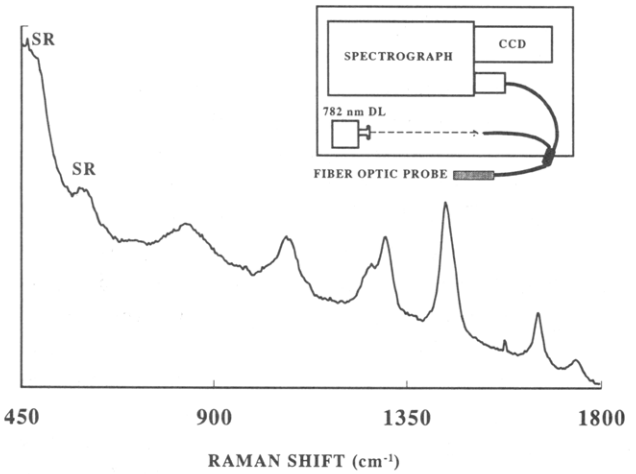

Figure 9. Raman spectrum of normal breast tissue using a portable Raman spectrometer 782-nm diode laser excitation and a fiber optic probe taken at the Department of Anatomical Pathology, Emory University Hospital, Atlanta, GA. Spectral conditions were 300 l/mm (1.0-μm blaze) grating, 50-μm slit (6.7-cm^{-1} bandpass), 7 mW, and 60 s of integration. The bands labeled SR are due to silica Raman bands from the fiber optic probe.

CONCLUSIONS

The overall objective of the experiments described here was to evaluate the utility of near-IR Raman spectroscopy for characterizing human tissue and to determine the principal molecular components in breast tissue responsible for these Raman features. In the context of these objectives, several conclusions deserve note. First, near-IR laser wavelengths in the 691–832-nm range yield high S/N spectra with moderate laser power. Background luminescence was significantly lower in these samples when red/near-IR excitation instead of visible excitation was used. Second, the laser wavelength can be manipulated to select for different tissue components, with visible lasers enhancing carotenoids and near-IR lasers producing mainly lipid bands. Third, of the major lipid bands identified in normal tissue, oleic acid appears to be the principle component observed. Fourth, fiber optic sampling is feasible, making this technique potentially valuable in the clinical setting with in vivo detection conceivable. The apparatus described in Figure 9 is a prototype of a commercially available instrument, and the user need not have extensive Raman experience to obtain useful spectra. More powerful diode lasers and thermoelectrically cooled CCD detectors are already commercially available, thus improving sensitivity and reducing instrumental complexity.

Even though surgical specimens of breast tissue were obtained for reasons varying from breast enlargement to breast cancer, all of the features reported here for normal breast tissue were qualitatively similar from sample to sample. Thus, we noted no qualitative differences between normal tissue removed for recontouring a large breast and normal tissue adjacent to but not involved by a breast cancer. Large groups of breast tissue specimens from patients with particular disease states were not available to accurately evaluate changes in peak areas or intensities associated with each disease. We are currently examining such groups in order to assess possible diagnostic utility of Raman spectroscopy. The current report serves as an initial characterization of Raman-observable components of normal breast biopsy tissue, and subsequent studies comparing normal to diseased tissue are underway.

ACKNOWLEDGMENT

This work was supported by the Analytical and Surface Chemistry section of the National Science Foundation. The authors also acknowledge the loan of equipment from Chromex (Albuquerque, NM).

Received for review September 16, 1993. Accepted November 15, 1993.®

• Abstract published in *Advance ACS Abstracts,* December 15, 1993.